ORIGINAL PAPER

CrossMark

Design and development of a 5 DOFs robotic surgical instrument with a force feedback for RAMIS

K. B. Karthikeyan[1] · V. Nithya[2]

Abstract

In this paper we report the conceptual design, fabrication and validation of a surgical robotic instrument for robotic assisted minimally invasive surgery. Medical practitioners are involved in all the phases of the interactive design and prototyping of the instrument. The instrument design parameters are derived from the surgeon's needs such as compactness with 5 mm thickness, 5 Degrees of Freedom (DOFs) to provide a wrist-like movement inside the surgical cavity and the force feedback to obtain the feel of touch. The instrument tip has a jaw like structure to support the tissue gripping. We achieved the opening and closing of this jaw with the help of a shape memory alloy (SMA). A force sensor placed near the SMA captures the forces as low as 570 mN from the surgical environment to provide the force feedback to the surgeon. This rigid body surgical instrument exerts an adequate force required for high force demanding applications such as suturing and needle insertion. In addition, we demonstrate a 4 DOFs serial robotic slave manipulator which carries the surgical instrument as an end effector. This report paves the way towards the development and commercialization of low-cost, compact and stable surgical robotic instrument and its manipulator for biomedical applications.

Keywords Surgical robot · Shape memory alloy · Force feedback · Force sensor

1 Introduction

Recently, surgical robotics became an important advancement in the field of medicine. Robotics assisted minimally invasive surgery (RAMIS) has attained the worldwide acceptance due to less operative traumatic harm without compromising the benefits of a conventional surgery [1]. In RAMIS, the robot assists the surgeon to perform the surgery by virtually replacing the surgeon from the surgical environment (0.5–2 m away). RAMIS consists of two major parts named master and slave, where the master controls the slave using a bidirectional controller [2,3]. This paper elaborates about the surgical slave robot which consists of a manipulator and an endoscopic instrument (see Fig. 1a, b) to perform the surgery inside a human body as instructed by the surgeon.
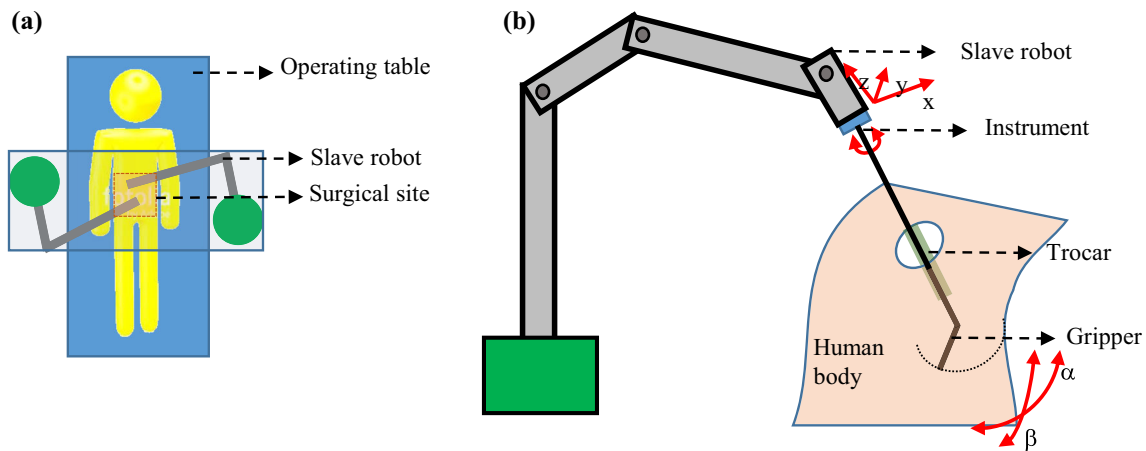
As a part of this work, many interactive studies were conducted among the medical practitioners. As per their suggestion, the robotic surgical instrument should be ultra-thin and light weight such that the surgeon can access the surgical cavity with a lesser tissue trauma. It was also noted that a wrist like movement of the surgical tip in the instrument is essential during the surgery to easily manoeuvre inside the surgical site. Commercial surgical instruments developed by various companies like DaVinci [4], Zeus [5], Miro-surge [6] and SOFIE [7] are bulky, complex and expensive. Later, the researchers focused on the development of thin instruments with continuum joints [8] but these instruments failed during the high force demanding applications such as suturing and needle insertion [9,10]. Also, in commercial surgical instruments, the surgeons perform the surgery with a hand-eye coordination that is, a visual feedback [11,12]. An additional force feedback from the surgical instrument is beneficial to the surgeon during a robotic surgery to sense the feel of touch. Zhou et al. investigated the effect of haptic feedback for suturing which suggests that the force feedback provides consistent and quick learning curve to the surgeon

✉ V. Nithya
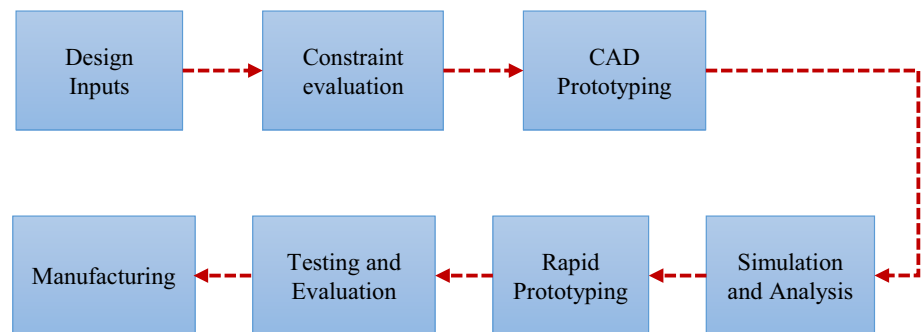 nithya.v@vit.ac.in

  K. B. Karthikeyan
  kbkarthikeyan@gmail.com

[1] School of Electronics Engineering, VIT, Chennai Campus, Chennai, India

[2] School of Electrical Engineering, VIT, Chennai Campus, Chennai, India

(a)

Operating table

Slave robot
Surgical site

(b)

Slave robot

Instrument

Trocar

Gripper

Human body

α

β

Fig. 1 **a** Schematic representation of RAMIS and **b** slave robot with surgical instrument as an end-effector

Fig. 2 Design framework

Design Inputs → Constraint evaluation → CAD Prototyping

Manufacturing ← Testing and Evaluation ← Rapid Prototyping ← Simulation and Analysis

[13]. Later, Song et al. reported 3 degrees of freedom (DOFs) force sensing for the surgical procedure to measure forces due to uncertainties like tissue trauma [14]. Therefore, the force feedback is essential in RAMIS to enhance the surgical skills and to reduce surgical procedural time. However, till this date, the instruments developed with force feedback are either complex or fails during the sterilization process. The proposed design described in this paper on the robotic instrument combined with the 4 DOFs slave robot satisfies the requirements of the medical practitioners.

The requirements of less mechanical amplifiers near the gripper for an optimized output and the complexities in its manufacturing possibilities are the real challenges in the design of this instrument. The Computer Aided Design (CAD) helped to visualize and study the instrument and the slave robot virtually before finalizing the design [15,16]. Simulation studies were performed to obtain optimized results for positioning the force sensor near the gripper, the action of the shape memory alloy (SMA) and to evaluate the force performance parameters. The process and the material choice also had a critical impact in the prototyping of the slave instrument. Once the CAD design and simulation studies were finalized, using rapid prototyping technology (3 Dimensional printing) the instrument and slave robot design was validated to improve the reliability and quality in the final product such as shape and surface finish.

Later, experiments were conducted to validate the instrument's force sensing capability using various polymers which can help the surgeon to feel the tissue under interaction during a surgery. This instrument can also exert a force of ≈ 4.5 N, required for the high force demanding applications like suturing and needle insertion. In this paper, we also demonstrate a 4 DOFs serial robotic slave manipulator which carries the surgical instrument as an end effector. This slave robot along with the instrument can be placed on the surgical table to achieve the position (x, y and z) and orientation (α and β) as directed by the surgeon (see Fig. 1b) from his console to perform the robotic assisted surgery.

2 Design of instrument

2.1 Instrument design framework

Figure 2 depicts the block diagram representation of the interactive design framework of the instrument and its slave robot. This framework is devised from the knowledge based approach [15], which minimizes the cost and time of development in the instrument and the slave robot. In the initial development stage of these devices, the valuable inputs such as thickness, weight and force feedback requirements were considered from the surgeons to avoid tissue trauma and also
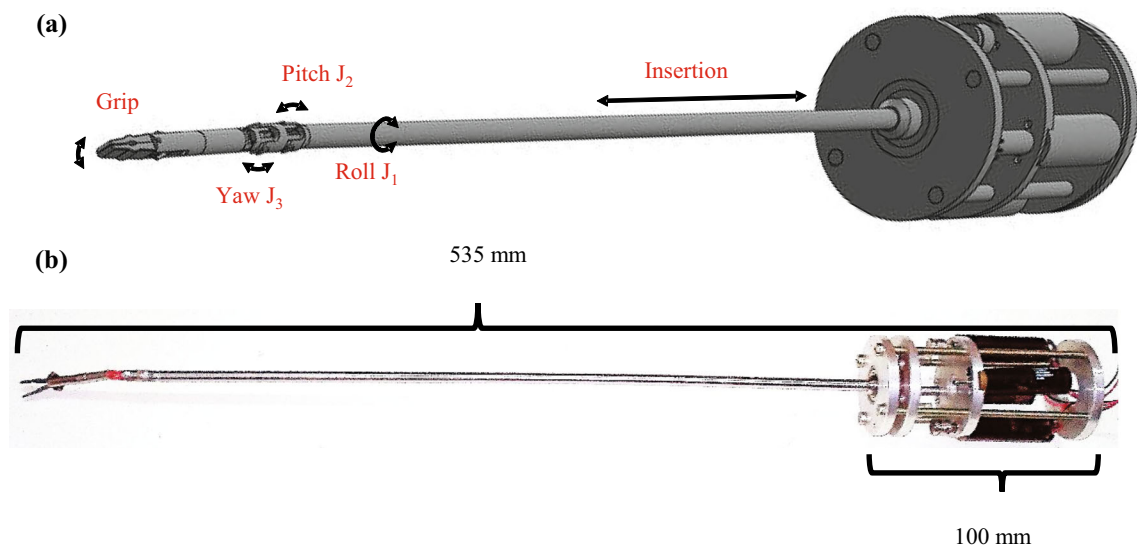
Fig. 3 **a** 3D conceptual design 5 DOFs surgical instrument and **b** manufactured 5 DOFs surgical instrument

to increase the efficiency of the surgery. These features helped to identify the constraints in the device which consequently lead to a 3D model implementation. Later, the simulation and Finite Element Analysis (FEA) of the proposed instrument design reveals the strength, accessibility, durability and sustainability of the instrument. Hardware implementation of the prototype validates the experimental results with the help of the controllers to a smooth controlled transient and stability.

2.2 Instrument overview

The surgical instrument is the critical component in RAMIS since it performs the surgery as commanded by the surgeon. An ultra-thin instrument is necessary for the surgeon to access the surgical cavity in the patient with a lesser tissue trauma. The instrument is inserted into the human body with help of a 6 mm trocar. As discussed before, the surgical instrument was first modeled with help of CAD as shown in Fig. 3a. Figure 3b shows the actual surgical instrument developed for RAMIS with 5 mm diameter. In this work, the final instrument was manufactured using stainless steel because it provides better strength and stability when forces are applied. This sterilizable material is non-reactive to any chemicals or temperatures during the surgery. Table 1 gives the physical dimensions of the instrument and the slave robot. The design of the instrument consists of a drive mechanism, transmission rod and a gripper as depicted in Fig. 4.

2.3 Drive mechanism

The drive mechanism is the top most part of the instrument with a cylindrical shape having a diameter of 50 mm and length of 100 mm. This part of the instrument consists of four

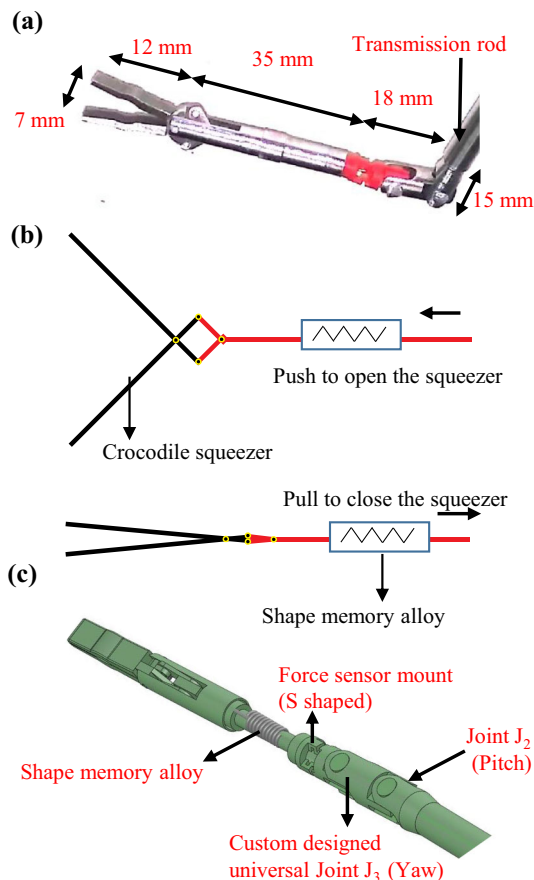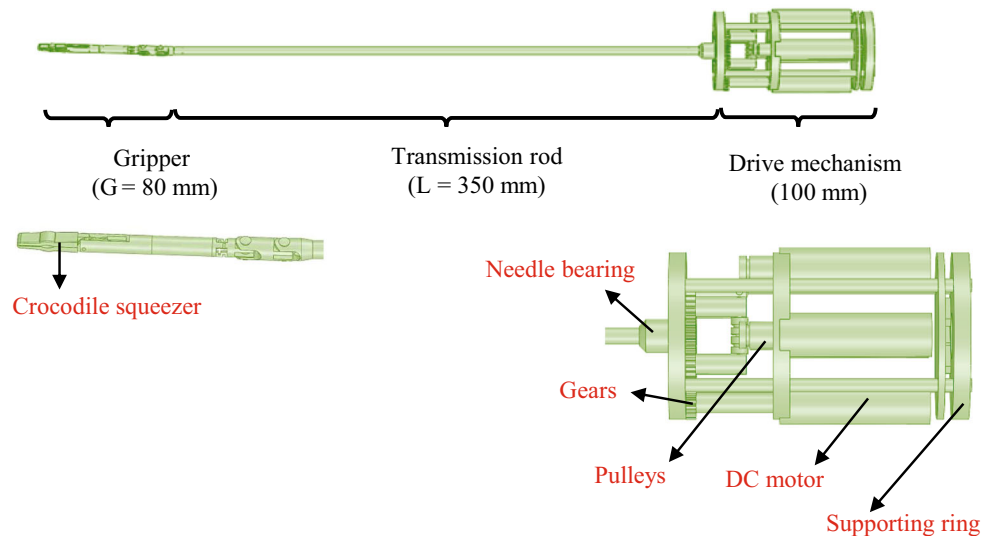**Table 1** Instrument properties

Instrument	Height	535 mm
	Width near drive	100 mm
	Width near tip	5 mm
	Weight	295 gms
Robot	Height	1250 mm
	Weight	4000 gms

DC motors (Maxon series) to drive the instrument's tip to the commanded positions inside a surgical cavity. In addition, the drive mechanism has pulleys, gears and supporting rings (see Fig. 4) to enable gripping motion [17]. The supporting rings hold the superstructure of the instrument which further connects to the 350 mm long (L) transmission rod to deliver the required torque to the gripper via Ni-Ti cable (0.5 mm). Small collars are placed inside the transmission rod to avoid buckling in the cable.

2.4 Gripper

The gripper is the most crucial part in the instrument, which interacts with the tissue of the human body during a surgical procedure. After several iterations, the gripper was finalized to have a length of G = 80 mm. The gripper has the capability to swivel in any direction like a wrist, using 5 DOFs namely roll (joint J_1), pitch (joint J_2), yaw (joint J_3) (see Fig. 3a), insertion and gripping. This interactive design of the instrument helped to obtain efficient dexterity inside the surgical cavity. Here, the length of the gripper tip to the joint J_3 is selected as $l_g = 65$ mm, whereas the length between the transmission rod to the joint J_3 is $l_j = 15$ mm which is

Fig. 4 The 3D model of the instrument

(a)

(b)

Push to open the squeezer

Crocodile squeezer

Pull to close the squeezer

Shape memory alloy

(c)

Fig. 5 **a** Dimensions of the gripper, **b** working principle of the shape memory alloy and **c** position of the force sensor mount

shown in Fig. 5a. This gripper has a jaw (upper and lower) with an identical size $l_c = 12$ mm, which has the shape of a crocodile squeezer for better gripping as depicted in Fig. 5a. The jaw is connected to the Ni–Ti cable to the DC motors through a tiny hollow chamber enclosed with a SMA [18].

The SMA has 10 thin coils of 15 mm length and 2.5 mm diameter, which is made up of stainless steel to enable the gripping action of the instrument. The SMA contracts and expands with the help of a DC motor to perform the gripping action as indicated in Fig. 5b.

The force sensors were implanted on the S-shaped mount (see Fig. 5c) near the SMA to capture the forces from the surgical environment. Figure 5(c) also shows the custom designed universal joint (which is an additional DOF to the previous demonstration [17]) to improve the accessibility of the gripper. Further, the custom designed universal joint was connected to a second universal joint to allow the gripper swivel seamlessly to any position inside the surgical cavity (analyzed in the kinematics section).

3 Kinematics analysis

Kinematics is used to perform the mathematical analysis of the surgical instrument. Homogenous transformation matrix gives the forward and inverse kinematics relations of this instrument design.

3.1 Kinematics design of the instrument

In this design, the joint J_1 rotates at an angle θ_1 which is a roll, whereas joint J_2 gives the wrist like movement at an angle θ_2 called pitch and an extra joint J_3 at an angle θ_3 is named as yaw (see Fig. 3a), along with the insertion and gripping. As mentioned previously, the DC motors from the drive mechanism deliver necessary torque to the gripper for its actions. Deravit–Hartenberg (D–H) parameters of the instrument for the joints are given in Table 2. Homogeneous transformation matrix derived from D–H parameters are given in Eq. 1 [18]

Table 2 D–H Parameters of the instrument

i	α_{i-1}	a_{i-1}	d_{i-1}	θ_{i-1}
1	$\pi/2$	0	0	θ_1
2	0	l_j	0	θ_2
3	0	l_g	0	θ_3

$$^0_3T = \begin{bmatrix} c_1c_{23} & -c_1s_{23} & s_1 & c_1(l_gc_{23}+l_jc_2) \\ s_1c_{23} & -s_1s_{23} & -c_1 & s_1(l_gc_{23}+l_jc_2) \\ s_{23} & c_{23} & 0 & l_gs_{23}+l_js_2 \\ 0 & 0 & 0 & 1 \end{bmatrix} \quad (1)$$

where, $c_1 = \cos\theta_1$, $s_1 = \sin\theta_1$, $c_2 = \cos\theta_2$, $s_2 = \sin\theta_2$, $c_{23} = \cos(\theta_2 + \theta_3)$ and $s_{23} = \sin(\theta_2 + \theta_3)$.

The simulated 3 dimensional (3D) workspace of the instrument from Eq. 1 is shown in Fig. 6a. This figure illustrates that, both gripper and transmission rod rotates at $\pm 180°$ inside the surgical cavity while performing the RAMIS. However, in practical applications, the gripper rotation was limited to $\pm 150°$ due to the mechanical constraints in the instrument. The maximum workspace of the instrument inside the surgical cavity is ± 80 mm as shown in Fig. 6b.

3.2 Jacobian of the instrument

$$[\tau] = [J_s]^T \cdot [F] \quad (2)$$

The Eq. 2 gives the necessary torque information of the instrument. The Jacobian of the instrument J_s is shown in Eq. 3 [17], which is used to steer the instrument to the right location at right time (derived from Eq. 1). The instrument is later mounted onto a surgical slave robot which is detailed in the next section.
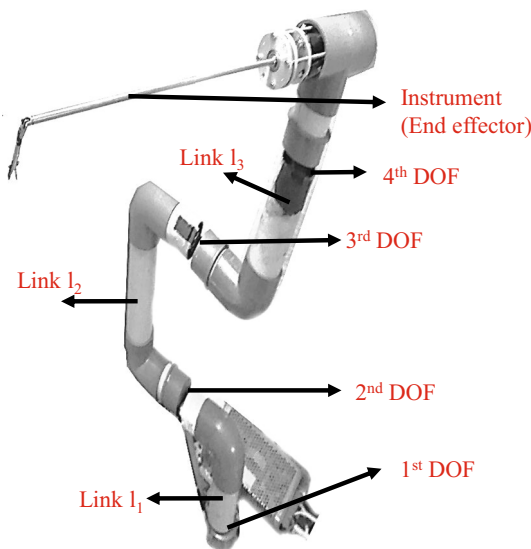

Fig. 7 Slave surgical robot with the end effector to perform RAMIS

$$J_s = \begin{bmatrix} -s_1(l_gc_{23}+l_jc_2) & c_1(l_gc_{23}+l_jc_2) & -l_gc_1s_{23} \\ c_1(l_gc_{23}+l_jc_2) & -s_1(l_gs_{23}+l_js_2) & -l_gs_1s_{23} \\ 0 & l_gc_{23}+l_jc_2 & l_gc_{23} \\ 0 & s_1 & s_1 \\ 0 & -c_1 & -c_1 \\ 1 & 0 & 0 \end{bmatrix} \quad (3)$$

4 Robotic slave manipulator

The 4 DOFs slave robot is an important segment in surgical robotics which holds the instrument as an end effector at a fixed tilt angle of $\beta = 60°$ as shown in Fig. 7. This
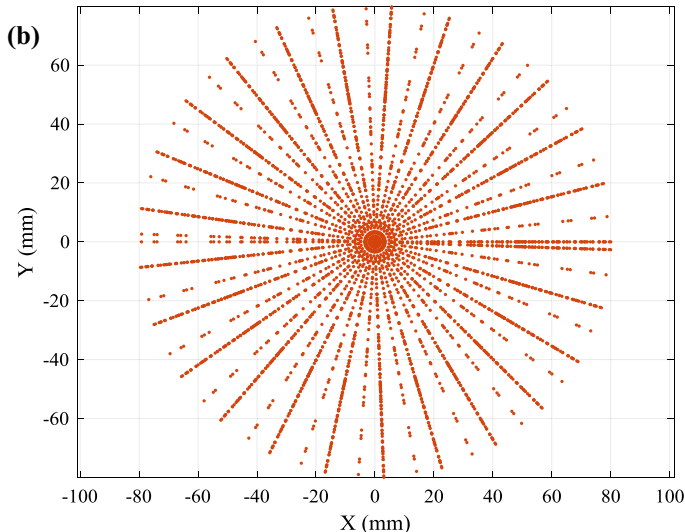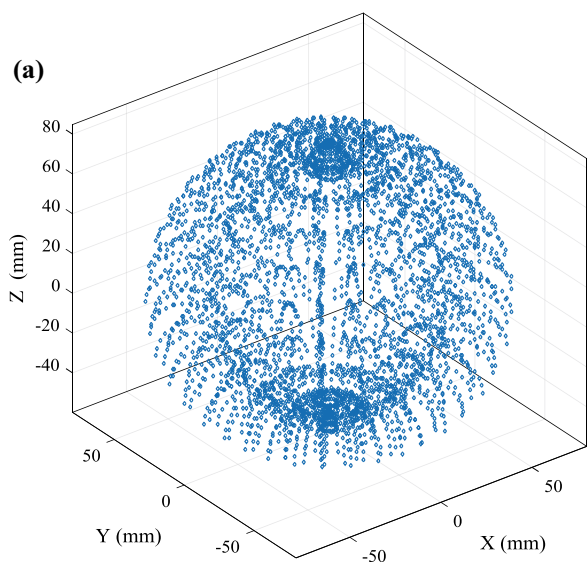
Fig. 6 **a** 3D workspace of the 5 DOFs gripper and **b** maximum limits of the gripper inside the surgical cavity

Table 3 D–H parameters of the 4 DOF serial robot

i	α_{i-1}	a_{i-1}	d_{i-1}	θ_{i-1}
1	$-\pi/2$	0	0	θ_1
2	0	l_1	0	θ_2
3	0	l_2	0	θ_3
4	$\pi/2$	l_3	0	θ_4

where,

$$n_x = c_1 c_{234} \quad o_x = -c_1 s_2 - s_1 \quad a_x = -c_1 s_{234}$$
$$p_x = l_3 c_1 c_{234} + l_3 c_1 c_{23} + l_2 c_1 c_2$$
$$n_y = s_1 c_{234} \quad o_y = -s_1 s_2 + c_2 \quad a_y = -s_1 s_{234}$$
$$p_y = l_3 s_1 c_{234} + l_3 s_1 c_{23} + l_2 s_1 c_2$$
$$n_z = s_{234} \quad o_z = c_2 \quad a_z = c_{234}$$
$$p_z = l_3 s_{234} + l_3 s_{23} + l_2 s_2$$

virtually separates the surgeon from the surgical table and gives the comfort, accessibility and dexterity to the surgeon. In this paper, the designed slave robot has 4 DOFs to place the instrument in three major positions and one orientation (x, y, z and α) [19]. The D–H parameters given in Table 3 helps us to visualize the slave robot mathematically. Equation 4 gives the homogeneous transformation matrix of the slave robot to find the position and orientation of the instrument using kinematics [19].

$$
{}^0_4T = \begin{bmatrix} n_x & o_x & a_x & p_x \\ n_y & o_y & a_y & p_y \\ n_z & o_z & a_z & p_z \\ 0 & 0 & 0 & 1 \end{bmatrix} \tag{4}
$$

5 Control system

Figure 8(a) shows the electronics of the instrument. It has a bilateral controller ATMega328P to control both the position and force of the instrument. L298D is used as the motor amplifier to drive the DC motors in the instrument. The position controller k_s obtains the commanded position x_s and steers the gripper accordingly inside the surgical cavity. Meanwhile, the force controller captures the forces f_e acting on the gripper from the surgical environment and transfers it to the surgeon to realize the force-feedback.

Fig. 8 **a** Hardware circuitry for the instrument and **b** the controller block diagram
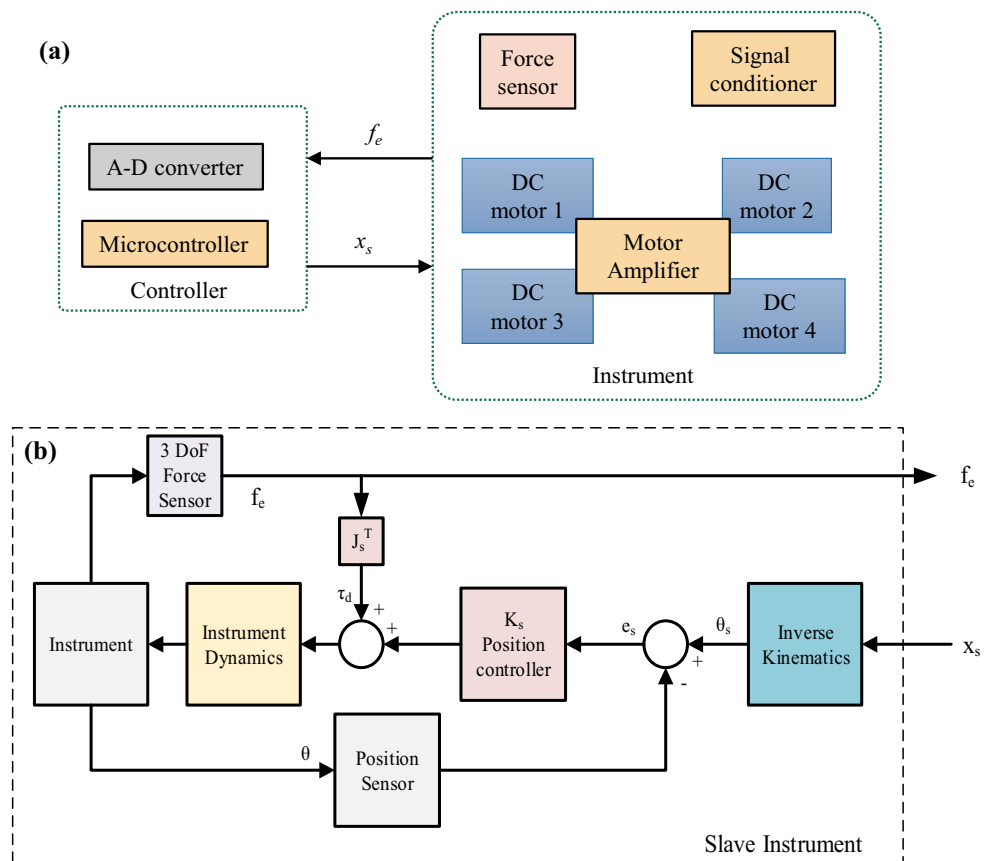
Fig. 9 **a** S-shaped force sensor mount, **b** FEA of the force sensor for stress and **c** placement of the sensor mount
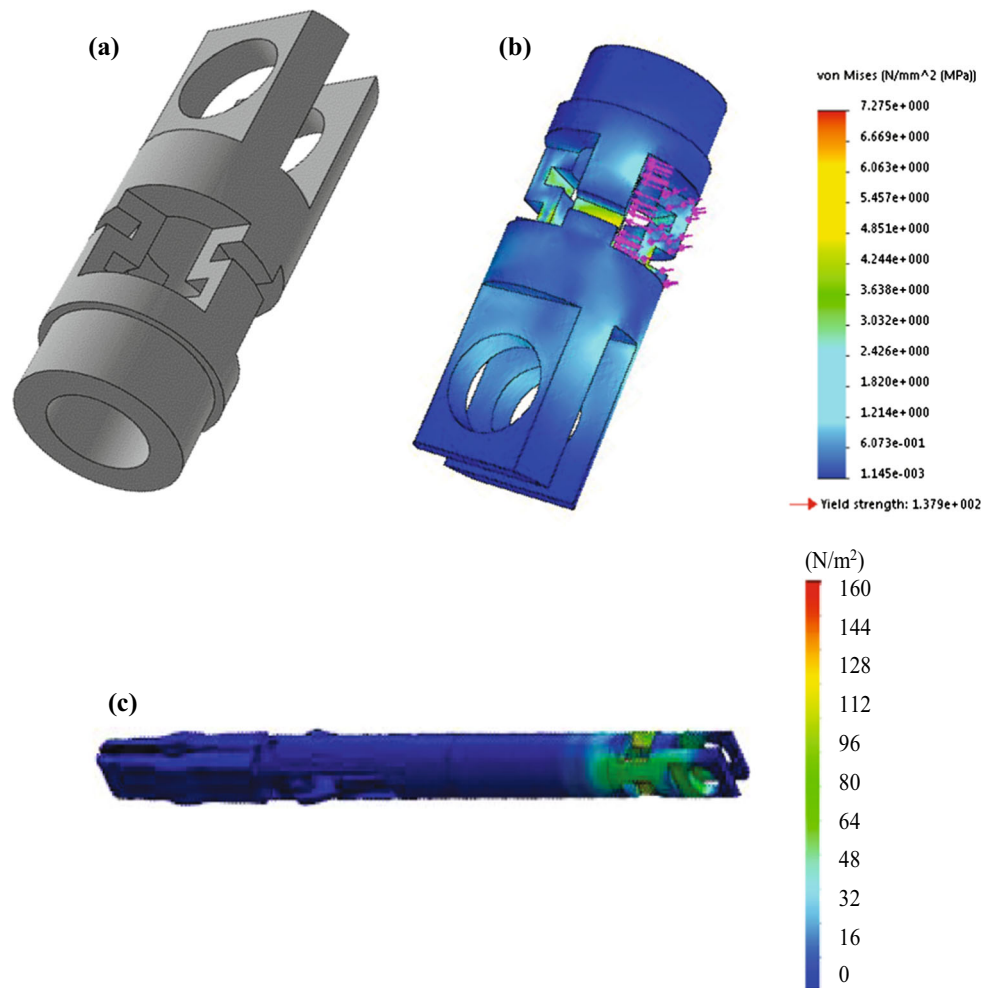
5.1 Position control

The controller block diagram is shown in Fig. 8b. This shows the joints $[J_1, J_2, J_3]^T$ are controlled correspondingly to position the gripper to $[\theta_1, \theta_2, \theta_3]^T$. The error signal e_s modulates the voltage or pulse width modulation (PWM) to control the DC motors. Proportional derivative (PD) controller or k_s is used to maintain the controller as a true follower to the commanded position and also provide adequate stiffness. The experimentally obtained controller gains, $k_p = 3.2$ and $k_d = 0.0181$ are used to ensure stability, smooth transient in DC motors, repeatability and stiffness of the surgical instrument.

5.2 Force control

The force controller captures the 3D forces acting on the instrument from the surgical environment. This helps the surgeon to realize the force-feedback from the obtained forces f_e. The shape and placement of the sensor mount on the surgical instrument is critical since it has to acquire the tissue interaction and the nonlinearities due to accidental contacts in the surgical cavity. The FEA gives a visual representation of the force or stress gradients as well as paves a way to rapidly analyze the modifications in the instrument design. In this work, FEA is used to estimate the position of the force sensor mount on the instrument to capture the forces from the surgical cavity. In order to initiate the FEA, we have first designed various components for the instrument based on the surgeon's requirements. Various iterations of the design were performed using FEA, until we find a suitable model which satisfies the surgeon's criteria. Once this interactive design of the instrument is finalized, it is rapid prototyped to test for its functionality.

As discussed before, the shape and positioning of the force sensor mount on the instrument was finalized using FEA. From simulations, it was noted that the most suitable sensor mount is a hollow cylindrical shaped rod with three 'S-shaped' pillars (see Fig. 9a) which helps to trap the forces from the surgical environment. Figure 9(b) depicts the forces of 1 N acting on the designed 'S-shaped' pillar of the force mount. This also shows the ability of the sensor mount to
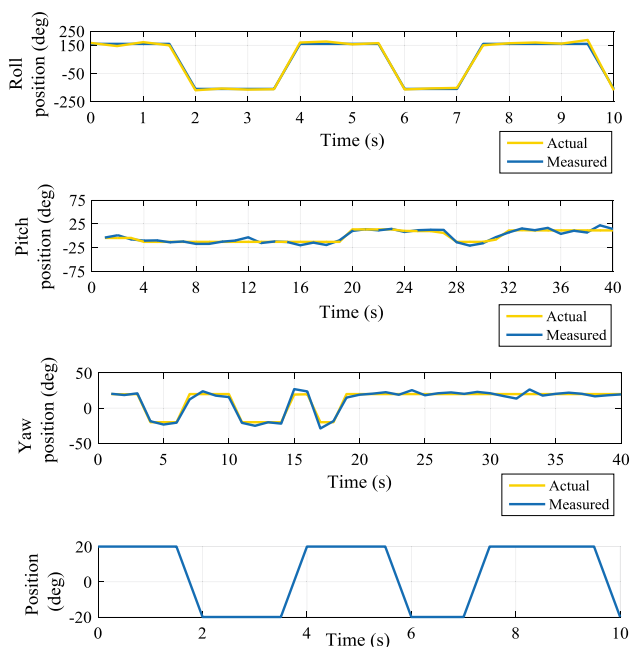
Fig. 10 Position control observation

Fig. 11 Force reflection from the force sensor

capture the forces from its pillars for any small stress caused on the surgical instrument. The FEA reveals that the better force reflection is obtained when the force sensor mount is placed in-between the SMA and universal joint as illustrated in Fig. 9c.

6 Results and discussions

The surgical instrument demonstrated in this paper has a bilateral data transfer to control both the position and force. The position is commanded by the surgeon from the surgeons console. Whereas the force from the surgical cavity is sent through the instrument to realize the force feedback by the surgeon at his console. Various signals were fed to the controller to analyze its stability and repeatability. Figure 10 shows the significance of the position controller for a smooth transient and stability of the DC motors. Each joint were individually analyzed to ensure the precision and accuracy of their motion. The roll joint J_1 seems to trace the test signal perfectly with a deviation of $\pm\,0.6°$ in its position, whereas the yaw joint J_2 and pitch J_3 joint has a time delay of 100 ms with a deviation $\pm\,0.9°$ in position. Therefore, a latency of 120 ms was observed in the surgical instrument, which can be due to the dimensional limitations of the instrument. Efforts are underway to optimize the instrument with a field programmable gate array to minimize this latency.

As discussed before, the force sensors were placed in the custom designed sensor mount which precisely captures the forces from the surgical cavity. During this experiment, exter-
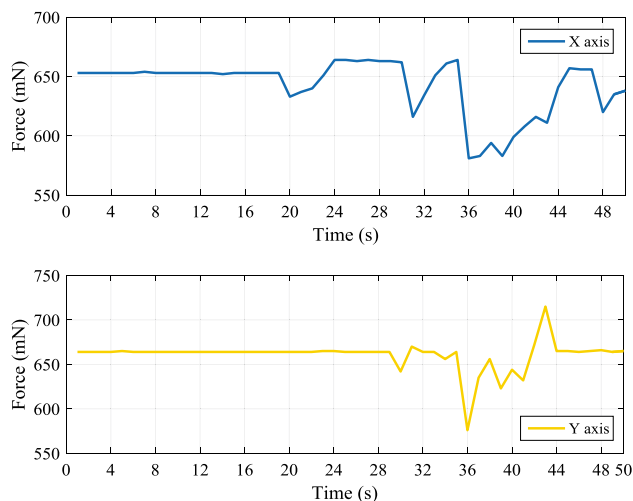
nal vibrations were introduced to the gripper as test signals at various levels to ensure the capability of the force sensor. Figure 11 shows the minimum measurable force feedback as 580 mN in the x-axis and 570 mN in y-axis when the tiny tremors acted on the instrument. This force-feedback clearly states that the surgeon can perceive any tiny tremors upto 570 mN while performing the surgery. It was also noted from the experiments that the instrument has the ability to exert a maximum force of 4.5 N at its gripper while executing the high force demanding applications such as suturing and needle insertion. The fabrication cost of the instrument and the slave robot was $250 and $300, respectively. The main challenge in designing and prototyping the instrument was the limited diameter of 5 mm. However, micro-fabrication helped to overcome this disadvantage to some extent. Later, the feedback from the user (surgeons) has given a positive note on this newly developed system and they have recommended it for biomedical testing. Whereas, the engineers (developers) could not maintain the minimum tolerance level and they were lacking precision by 10% while performing the micro-fabrication.

7 Conclusion

In conclusion, to the best of our knowledge, this is the first demonstration of low cost 5 DOFs ultra-thin (5 mm) rigid body robotic surgical instrument with a force feedback. As per the interactive design requirements of the medical practitioner, this instrument consists of fewer mechanical components near the gripper which significantly reduces the complexity, friction and procedural time while performing a laparoscopic surgery. This surgical instrument could sense the forces as low as 570 mN, which eventually helps the surgeon to feel the tissue under interaction during the surgery.

The instrument was later mounted onto a 4 DOFs slave robot as an end effector to enable the laparoscopic surgery. The designed slave robotic system is a promising method to obtain an advantageous interaction between the surgeon and the engineer. This demonstration paves way for the development of low cost surgical instruments with force feedback in the field of medical robotics.

References

1. Garcia-Ruiz, A., Gagner, M., Miller, J.H., Steiner, C.P., Hahn, J.F.: Manual versus robotically assisted laparoscopic surgery in the performance of basic manipulation and suturing tasks. Arch. Surg. **133**(9), 957–961 (1998)
2. Rosen, J., Hannaford, B.: Doc at a distance. IEEE Spectrum pp. 34–39 (2006)
3. Taylor, R.H., Stoianovici, D.: Medical robotics in computer integrated surgery. IEEE Trans. Rob. Autom. **19**(5), 765–781 (2003)
4. "Intuitive Surgical," [Online] Available. https://www.intuitivesurgical.com/
5. Reichenspurner, H., Demaino, R., Mack, M., Boehm, D., Gulbins, H., Detter, C., Meiser, B., Ellgass, R., Reichart, B.: Use of the voice controlled and computer-assisted surgical system Zeus for endoscopic coronary artery surgery bypass grafting. J. Thorac. Cardiovasc. Surg. **118**, 11–16 (1999)
6. Hagn, U., Ortmaier, T., Konietschke, R., Kbler, B., Seibold, U., Tobergte, A., Nickl, M., Joerg, S., Hirzinger, G.: Telemanipulators for remote minimally invasive surgery. IEEE Rob. Autom. Mag. (RAM) **15**(4), 28–38 (2008)
7. van den Bedem, L.J.M., Hendrix, R., Rosielle, P.C.J.N., Steinbuch, M., Nijmeijer, H.: Design of a minimally invasive surgical teleoperated master-slave system with haptic feedback. In: International Conference on Mechatronics and Automation (ICMA), pp. 60–65 (2009)
8. Tzemanaki, A. et al.: Design of a multi-DOF cable-driven mechanism of a miniature serial manipulator for robot-assisted minimally invasive surgery. In: 2016 6th IEEE International Conference on Biomedical Robotics and Biomechatronics (BioRob), Singapore, pp. 55–60 (2016)
9. Talasaz, A., Trejos, A.L., Patel, R.V.: Effect of force feedback on performance of robotics-assisted suturing. In: 2012 4th IEEE RAS & EMBS International Conference on Biomedical Robotics and Biomechatronics (BioRob), Rome, pp. 823–828 (2012)
10. Okamura, A.M., Simone, C., OLeary, M.D.: Force modelling for needle insertion into soft tissue. IEEE Trans. Biomed. Eng. **51**(10), 1707–1716 (2004)
11. Breedveld, P., Wentink, M.: Eye-hand coordination in laparoscopy an overview of experiments and supporting aids. Minim. Invasive Ther. Allied Technol. **10**(3), 155162 (2001)
12. Shoham, M., Burman, M., Zehavi, E., Joskowicz, L., Batkilin, E., Kunicher, Y.: Bone-mounted miniature robot for surgical procedures: concept and clinical applications. IEEE Trans. Rob. Autom. Special issue on Medical Robotics **19**(5), 893–901 (2003)
13. Zhou, M., Tse, S., Derevianko, A., Jones, D.B., Schwaitzberg, S.D., Cao, C.G.L.: The effect of haptic feedback on laparoscopic suturing and knot-tying: a learning curve study. In: Proceeding of the Human Factors and Ergonomics Society, pp. 880–884 (2008)
14. Qin, H., Song, A., Liu, Y., Jiang, G., Zhou, B.: Design and calibration of a new 6 DOF haptic device. Sensors (Basel, Switzerland) **15**(12), 31293–31313 (2015)
15. Mele, M., Campana, G.: Prediction of Kansei engineering features for bottle design by a Knowledge Based System. Int. J. Interact. Des. Manuf. (IJIDeM) (2018). https://doi.org/10.1007/s12008-018-0485-5
16. Naddeo, A., Califano, R., Vink, P.: The effect of posture, pressure and load distribution on (dis)comfort perceived by students seated on school chairs. Int. J. Interact. Des. Manuf. (IJIDeM) (2018). https://doi.org/10.1007/s12008-018-0479-3
17. Karthikeyan, K.B., Nithya, V.: Implementation of surgical robot instrument with a force feedback. In: IEEE Region 10 Humanitarian Technology Conference (R10-HTC), Dhaka, pp. 101–104 (2017)
18. Evangeliou, N., Tzes, A.: Development of an SMA-actuated redundant robotic platform for minimally invasive surgery. In: 2016 6th IEEE International Conference on Biomedical Robotics and Biomechatronics (BioRob), Singapore, pp. 353–358 (2016)
19. Craig, J.J.: Introduction to robotics: mechanics and control. Pearson/Prentice Hall, Upper Saddle River, NJ, USA (2005)